Synergistic adsorption of phenol from aqueous solution onto polymeric adsorbents

Zhang W. Ming, Chen J. Long [*], Pan B. Cai, Zhang Q. Xing, B. Zhang

State Key Laboratory of Pollution Control and Resources Reuse, School of the Environment, Nanjing University, Nanjing 210093, PR China

Abstract

Adsorption of phenol from aqueous solution onto a nonpolar adsorbent, aminated adsorbent and weak base adsorbent (Amberlite XAD4, NDA103 and Amberlite IRA96C, respectively) at temperatures from 293 to 313 K was studied for the weak interactions between the phenol molecules and the polymeric adsorbents. Isotherms of Langmuir and Freundlich equation with characteristic parameters for different adsorbents were well fitted to the batch equilibrium adsorption data. The adsorption capacity on NDA103 driven by hydrogen bonding and van der Waals interaction together is higher than that on IRA96C driven by hydrogen bonding interaction only and on XAD4 driven by van der Waals interaction only. For evaluating synergistic adsorption for phenol–water systems onto polymeric adsorbents, the adsorption capacity is normalized to the amounts of specific surface area and amino groups of adsorbents. The synergistic effect with other weak interactions would contribute more to the adsorption as acting simultaneously than that of acting individually.
© 2005 Elsevier B.V. All rights reserved.

Keywords: Polymeric adsorbent; Phenol; Adsorption behavior; Synergistic effect

1. Introduction

Contamination of surface water and groundwater with aromatic compounds is one of the most serious environmental problems human being faces today. Owing to its acute toxicity and good solubility, phenol has already been listed as one of the top priority contaminants and also the most important substructure of potentially carcinogenic pollutants discharged from fine chemical plants. Therefore, the efficient removal of phenol from waste streams has increasingly become a significant environmental concern [1,2]. Now many water treatment technologies are available to remove phenol from receiving water body including biological degradation, chemical oxidation and adsorption on activated carbon. In the past two decades, polymeric adsorbents have been viewed as a practical alternative to activated carbon for efficient removal of aromatic pollutants from wastewater [3–6], and adsorption mechanism of target compounds on polymeric adsorbents is of great interest today.

For phenol adsorption on a specific polymeric adsorbent, the solute–adsorbent interaction will play an important role in the adsorption capacity from aqueous solution. For a commercially available polymeric adsorbent, such as XAD4, it is generally known that van der Waals interaction is the main force to drive phenol molecules from bulk solution to adsorbent phase [6]. Also, hydrogen bonding interaction was taken as another driving force in some cases including phenol adsorption on a weakly anion exchanger [7–10]. In order to enhance adsorption capacity, scientists have now made much effort on chemical modification of polymeric adsorbents to improve their adsorption properties and some mechanisms have been reported to elucidate the adsorption enhancement on the functionalized adsorbents [11–14]. But study on the synergistic effect, which arises from more than two types of driving forces occur simultaneously on a specific polymeric adsorbent, is still scarce [15,16].

---

* Corresponding author. Tel.: +86 25 83596731; fax: +86 25 83596731.
  E-mail address: zwmnju@sina.com (C.J. Long).

Table 1
Physical properties of phenol at 298 K [4]

Adsorbate	Phenol
Surface area (nm^2/molecule)	0.305
Cross-sectional distance (nm)	0.43
Saturated concentration in water, C_s (mol/m^3)	925
pK_a	9.89

In this paper, a newly developed adsorbent NDA103 with amino group on the polymeric matrix was employed to mimic the multiple weak interactions on phenol adsorption from aqueous solution. Through batch phenol adsorption runs on XAD4, NDA103 and a weakly anion exchanger IRA96C, the present work was aimed at achieving a better understanding on the interactions of phenol and adsorbent and elucidating the synergistic mechanism of weak interactions.

2. Experimental studies

Phenol (analytical grade) was purchased from the Shanghai Chemical Reagent Station (Shanghai, PR China) and used in the study without further purification. Phenol was dissolved in deionized water in the batch adsorption runs without pH adjustment. Some physiochemical properties of phenol are presented in Table 1.

Amberlite XAD4 (a nonpolar adsorbent) and IRA96C (a weak base adsorbent) were purchased from Rohm & Haas (Philadelphia, PA, USA), while NDA103 (an aminated adsorbent developed by our research group) was produced in Langfang Electrical Resin Co. Ltd. (Hebei Province, PR China).

Batch adsorption tests were performed using the conventional bottle-point technique in 100 mL glass flasks at different temperatures (293, 303 and 313 K). Prior to use, all the adsorbents were extracted with ethanol for 8 h in a Soxhlet apparatus and vacuum desiccated at 325 K for 24 h. Fixed adsorbent dosages of 0.050 g were directly introduced into a 100 mL glass flask. Owing to its nonpolarity, XAD4 was necessarily wetted with 0.5 mL of methanol and then rinsed three times with deionized water before use. Subsequently, 50 mL of an aqueous solution of phenol with an initial concentration ranging from 0.15 to 2 mmol/L was added into each flask.

The flasks were then transferred into a G 25 model incubator shaker with thermostat (New Brunswick Scientific Co.

Inc.) at a given temperature and shaken under 150 rpm for 24 h. Note that adsorption reaches equilibrium in 24 h according to the preliminary kinetic study. The amount adsorbed of phenol can be calculated by the following equation:

$$Q_e = V_L \frac{(C_0 - C_e)}{W} \tag{1}$$

where C_0 and C_e denote the initial concentration (mmol/L) and the residual concentration at equilibrium (mmol/L), respectively, Q_e refers to the amount adsorbed of phenol on the adsorbents (mmol/g), V_L is the volume of the aqueous solution (mL) and W is the mass of dry adsorbents (g).

The solution concentrations were determined using high performance liquid chromatography (HPLC), which was connected to Waters 600 controller, Waters 600 pump and Waters 2487 Dual Absorbance UV detector at 274 nm (Waters, USA). Mobile phase was 0.1% $KH_2PO_4 \cdot H_2O$:methanol = 70:30 (v/v) and flow rate was 1 mL/min.

3. Results and discussion

3.1. Characterization of the polymeric adsorbents

The aminated polymeric adsorbents NDA103 was obtained by aminating a macroreticular polymeric adsorbent NDA100 with dimethylamine [10]. The specific surface area and the pore distribution of all the employed polymeric adsorbents were determined in dry state with a Micromeritics ASAP 2010 M surface area measurement instrument (Micromeritics Instrument, Norcros, USA). Infrared spectra were obtained from a Nexus 870 SX IR spectrometer (USA) with KBr pelletted samples. The basic exchange capacity was measured by titration with 0.1 mol/L HCl and NaOH solutions.

The characteristics of the polymeric adsorbents are listed in Table 2. IR spectra (not shown) indicates that the absorbance peaks at 2771 and 2816 cm^{-1} are for C–H stretching vibration of the methyl group connecting to tertiary amino group on NDA103 and IRA96C, the vibration peak for C–N bond being at 1261 cm^{-1}.

Table 2
Characteristic properties of XAD4, NDA103 and IRA96C

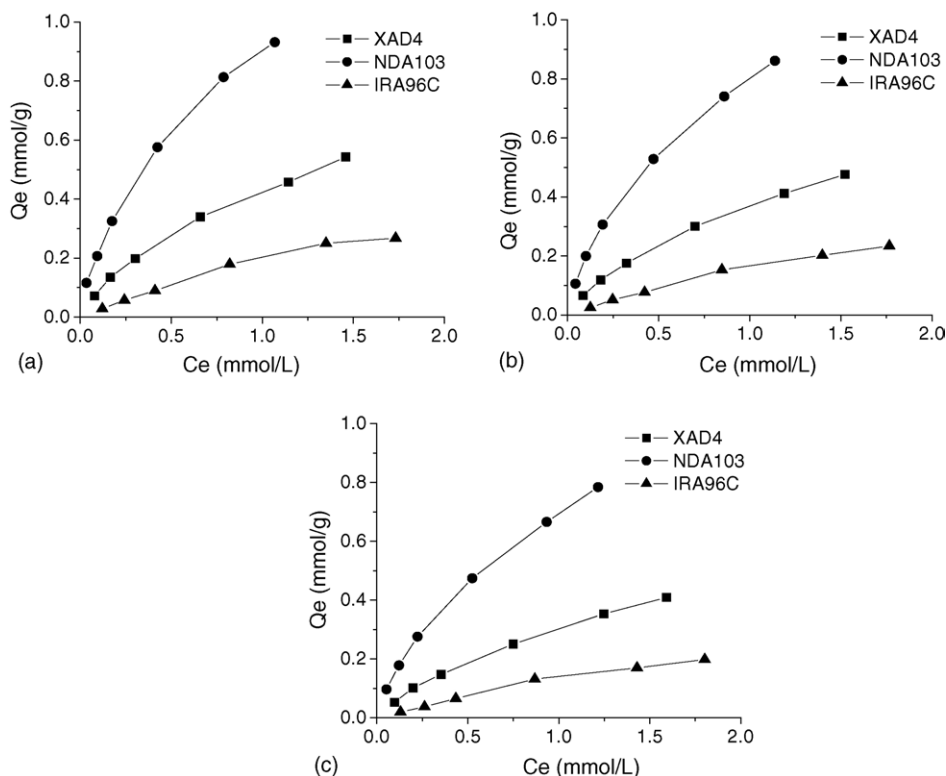| Property	XAD4	NDA103	IRA96C
Structure	Polystyrene	Aminated polystyrene	Weak base polystyrene
Polarity	Nonpolar	Moderately polar	Strong polar
BET surface area (m^2/g)	914	611	36
Average pore diameter (nm)	5.8	3.4	20.7
Desorption average pore diameter (nm)	8.4	17.6	30.5
Particle size (mm)	0.4–0.6	0.4–0.6	0.4–0.6
Tertiary amino group (mmol/g)	0	1.57	5.1
Colour	White	Deep brown	Yellow

Fig. 1. Equilibrium adsorption isotherms of phenol on adsorbents at: (a) 293 K, (b) 303 K and (c) 313 K.

3.2. Equilibrium adsorption

Adsorption isotherms of phenol on XAD4, NDA103 and IRA96C at desired temperatures (293, 303 and 313 K) are shown in Fig. 1(a–c), respectively. Adsorption of aromatic compounds on polymeric adsorbents has been successfully described by the Langmuir and Freundlich models [17,18]:

Langmuir equation $Q_e = \dfrac{Q_m K_L C_e}{1 + K_L C_e}$ (2)

Freundlich equation $Q_e = K_f C_e^{1/n}$ (3)

where Q_e is the amount adsorbed at equilibrium (mmol/g), C_e the equilibrium concentration in bulk fluid phase (mmol/L), Q_m the maximum adsorption capacity (mmol/g), namely

complete coverage of available adsorption sites, K_L the affinity constant, K_f an indicator of adsorption capacity, $1/n$ is related to the magnitude of the adsorption driving force and to the adsorbent site energy distribution.

The nonlinear least-squares regression was employed for data analyses and the results are presented in Table 3. It can be seen that both Langmuir and Freundlich isotherm models fit the adsorption data well since all the correlative factors R^2 are larger than 0.98 [19]. As concluded in Table 3, the constant n in the Freundlich isotherm is larger for NDA103 than for XAD4 and IRA96C, suggesting that NDA103 provides an relatively easier access for the phenol molecule to interact with the active sites in comparison with XAD4 and IRA96C. It can also be seen that the order of both K_f and Q_m for phenol adsorption is in order NDA103 > XAD4 > IRA96C,

Table 3
Adsorption isotherms of phenol on XAD4, NDA103 and IRA96C

| Adsorbent	Temperature (K)	Langmuir isotherm			Freundlich isotherm		
		K_L	Q_m	R^2	K_f	n	R^2
XAD4	293	0.910	0.926	0.995	0.426	1.560	0.998
	303	0.820	0.845	0.997	0.366	1.538	0.999
	313	0.639	0.800	0.997	0.300	1.457	0.999
NDA103	293	1.676	1.436	0.996	0.917	1.696	0.997
	303	1.517	1.330	0.995	0.806	1.672	0.998
	313	1.154	1.312	0.996	0.697	1.581	0.999
IRA96C	293	0.447	0.636	0.992	0.188	1.331	0.981
	303	0.420	0.552	0.997	0.156	1.328	0.990
	313	0.364	0.503	0.993	0.129	1.282	0.985
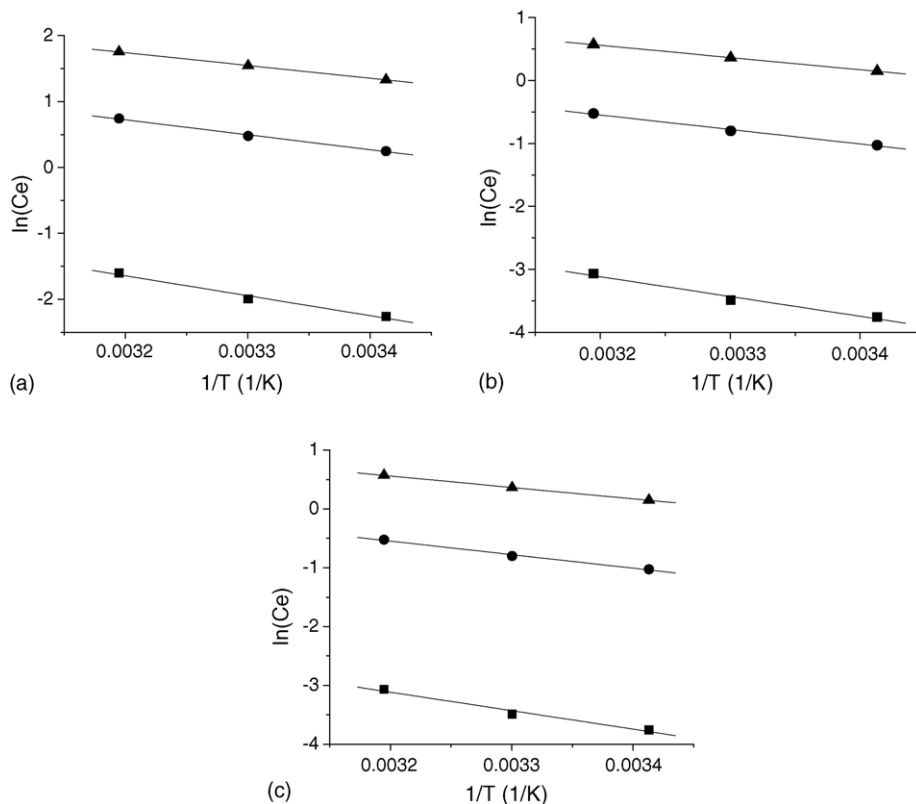
Fig. 2. van't Hoff plots (ln K vs. $1/T$) for the adsorption of phenol from aqueous solution onto: (a) XAD4, (b) NDA103 and (c) IRA96C at different Q_e values: ■, $Q_e = 0.1$ mmol/g adsorbent; ●, $Q_e = 0.5$ mmol/g adsorbent; ▲ and $Q_e = 1.0$ mmol/g adsorbent.

indicating the different adsorption affinities and adsorption capacities of phenol for the three adsorbents. The more excellent adsorption property of animated adsorbent NDA103 than IRA96C and XAD4 may be attributed to its much higher surface area with van der Waals interaction and partial amino groups on the structure with hydrogen bonding interaction, respectively. Additionally, the affinity of phenol towards the polymeric adsorbents is declined as the equilibrium concentrations increase. This is probably due to the reduction in the adsorption sites and the augment of the electrostatic repulsion caused by the increase in the negative charge of adsorbed phenol.

With respect to the effect of temperature, it is shown from Table 3 that the affinity constant (K_l) of phenol towards the tree adsorbents is declined as the temperature increases, indicating the exothermic nature, but the greater water affinity of phenol at higher temperature cannot be ruled out.

3.3. Thermodynamics of the adsorption

If isosteric sorption enthalpy change (ΔH) can be assumed to be approximately undependent on temperature, the followed equation could be given by van't Hoff equation [20]:

$$\frac{d(\ln C_e)}{d(1/T)} = -\frac{\Delta H}{R} \tag{4}$$

where T is the absolute temperature in K, R the gas constant, C_e the equilibrium concentration in bulk fluid phase inside the pores (mol/L) and ΔH is the isosteric sorption enthalpy change of adsorption. The enthalpy change can be computed from the slope of the $\ln C_e$ versus $1/T$ plot with the definite Q_e at different temperatures (293, 303 and 313 K). Examples of the curves obtained are depicted in Fig. 2(a–c).

The adsorption free energy changes can be calculated from the Freundlich isotherm by employing the Gibbs equation [20]:

$$\Delta G = -nRT \tag{5}$$

where n is the parameter of the Freundlich equation and ΔG is the free energy change on adsorption.

By above ways, the values of the isosteric enthalpy changes (ΔH) and the adsorption free energy changes (ΔG) computed from the experiment data in this study are presented in Table 4.

The negative values of ΔG in all cases indicate the spontaneous nature of phenol adsorption on the three adsorbents. Then the higher absolute value of the free energy changes is relative to the higher adsorption capacity, in agreement with the results obtained from an analysis of the adsorption isotherms. The enthalpy change ΔH for phenol adsorption on them are found to be also negative at the temperature from 293 to 313 K. The negative values confirm the exothermic nature of these adsorptions. Furthermore, their magnitudes

Table 4
Thermodynamic parameters for phenol on XAD4, NDA103 and IRA96C

Adsorbent	Q_e (mmol/g)	ΔH (kJ/mol)	ΔG (kJ/mol)		
			293 K	303 K	313 K
XAD4	0.1	−25.20	−3.80	−3.87	−3.79
	0.5	−18.86			
	1	−16.13			
NDA103	0.1	−26.22	−4.13	−4.21	−4.11
	0.5	−19.18			
	1	−16.16			
IRA96C	0.1	−19.80	−3.24	−3.35	−3.34
	0.5	−16.75			
	1	−15.44			

(<43 kJ/mol) show the driving force of the adsorption is mainly physical interaction. Further, the absolute values of ΔH decrease with increased loading, indicating that the active sites on the adsorbent surface are energetically heterogeneous and those of the greater binding energy are occupied firstly.

3.4. Synergistic effect on phenol adsorption on NDA103

In order to interpret the synergistic effect of phenol adsorption on polymeric adsorbents, NDA103 was introduced as the model adsorbent, while XAD4 and IRA96C were selected for comparative adsorbents. We assume that for a certain solute and solvent, different adsorption capacities of adsorbents were caused mainly by their different properties. The hydrophobic surface of the polymeric adsorbents could provide van der Waals interaction sites, while the tertiary amino groups could provide proton acceptors for hydrogen bonding

interaction, both of which could affect the adsorption capacity and attractive force. According to Table 2, the amount of the surface area of IRA96C (36 m^2/g) was much lower than that of NDA103 (611 m^2/g) or XAD4 (914 m^2/g), so the adsorption capacity contribution of van der Waals interaction can be negligible. As IRA96C contains much little van der Waals interaction site, hydrogen bonding interaction, if any, maybe the only interaction between the amino group on the structure of IRA96C and the hydroxyl group of phenol molecule. On the contrary, due to no amino group on the matrix of XAD4, the adsorption capacity contribution of hydrogen bonding interaction on XAD4 can also be negligible. Hence, we can assume that phenol adsorption on XAD4 is only driven by van der Waals interaction between the aromatic ring of phenol molecule and the phenyl ring on the matrix of XAD4. The adsorption of phenol on the comparative adsorbents, XAD4 and IRA96C, might be listed as the following schematic representation (Fig. 3(a and c)). Previous study [6,19] suggests that the adsorption capacity of nonpolar adsorbent is positive correlated with the amount of the specific surface area, while that of weak base, adsorbent is also positive correlated with the amount of the amino groups.

As seen from Tables 2–3, due to both some amino groups and large specific surface area, the driving forces of phenol on NDA103 are expected to include hydrogen bonding interaction and van der Waals interaction, which probably causes the greater adsorption capacity of NDA103 than XAD4 or IRA96C, though the amounts of specific surface area and tertiary amino groups of NDA103 are lower than XAD4 and IRA96C, respectively. However, whether the two interactions occur simultaneously with the same phenol molecule (chelating effect) and any synergistic effect exists between them is still unclear. If the two interactions occur synergistically, the
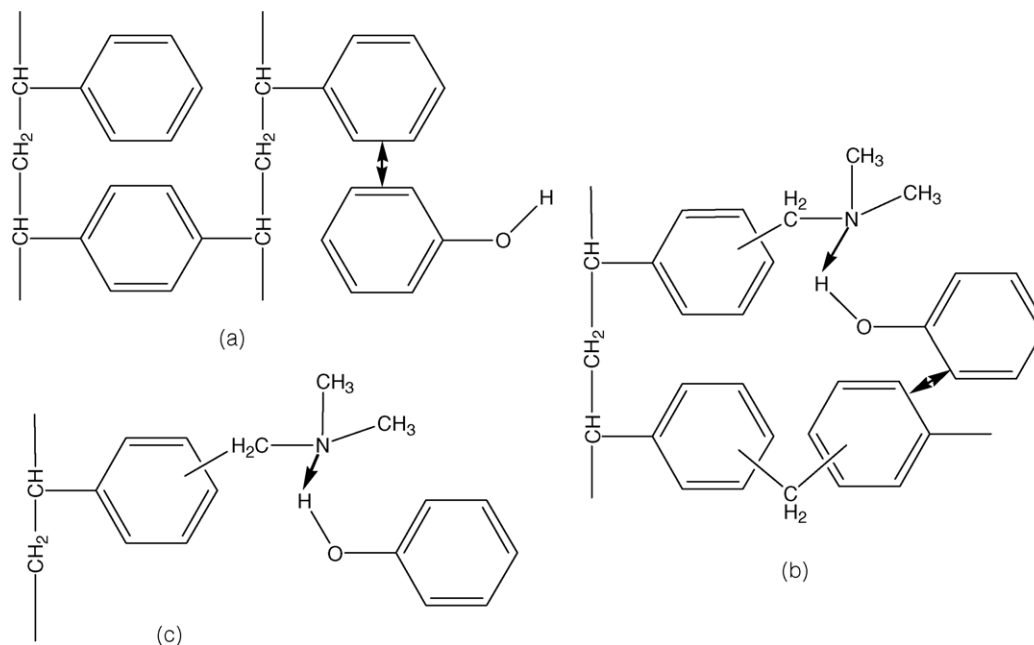

Fig. 3. Schemes for the chemical structure of adsorbents and the interactions between adsorbents and phenol.

Table 5
Synergistic effect for phenol adsorption capacities on NDA103

Temperature (K)	Q'_{mH} (mmol/g)	Q'_{mh} (mmol/g)	Q'_m (mmol/g)	Q_m (mmol/g)	R_e[a]	R
293	0.196	0.619	0.815	1.436	43.231	1.762
303	0.170	0.565	0.735	1.330	44.772	1.811
313	0.155	0.535	0.690	1.312	47.400	1.901

[a] Calculated by: $R_e = 100 \times (Q_m - Q'_{mh})/Q_m$.

adsorption results should meet the following two terms: (1) the adsorption affinity and adsorption free energy for the second interaction should be, respectively, higher and lower than that for the same interaction that occurs individually because the second interaction promotes the phenol molecule drawn from the bulk solution to the adsorbent phase, which is proved by the larger value of ΔG for NDA103 in Table 4 and (2) the total adsorption capacity should be much more than the sum of the two interactions that occur individually because the second interaction would be effectively intramolecular.

Given two assumptions: (1) van der Waals interaction and hydrogen bonding interaction act individually without any synergistic or competitive effect during the phenol adsorption on NDA103 and (2) van der Waals interaction is linear correlated with the amount of the specific surface area of nonpolar adsorbent normalized by XAD4, and hydrogen bonding interaction is linear correlated with the amount of the tertiary amino groups of weak base adsorbent normalized by IRA96C, the theoretical adsorption capacity of NDA103 can be decomposed completely by the adsorption contributions of the two interactions described as Eq. (4) and the synergistic effect can be quantitatively achieved.

$$Q'_m = Q'_{mh} + Q'_{mH} = S \times \alpha + G \times \beta \qquad (6)$$

where, Q'_m is the normalized theoretical adsorption capacity of NDA103 for phenol without any synergistic or competitive effect (mmol/g); Q'_{mh} and Q'_{mH} are the corresponding adsorption contributions of van der Waals interaction and hydrogen bonding interaction, respectively (mmol/g); α and β are the corresponding contribution coefficients of van der Waals interaction per unit surface area normalized by XAD4 and hydrogen bonding interaction per unit molar tertiary amino group normalized by IRA96C, respectively; S (m^2) and G (mol) are the amount of specific surface area and tertiary amino groups of NDA103, respectively. The theoretical and experimental values for phenol on NDA103 at saturation are listed in Table 5. It can be seen that the experimental adsorption capacity of phenol on NDA103 exceed to a large or small extent its theoretical one, indicating the total adsorption capacity is much more than the sum of van der Waals interaction and hydrogen bonding interaction that occur individually. Then it can be concluded that during the phenol adsorption process on NDA103, the two interactions occur simultaneously and synergistically, which might be listed in the schematic representation of Fig. 3(c).

To quantify the synergistic effect of van der Waals interaction and hydrogen bonding interaction on phenol adsorption
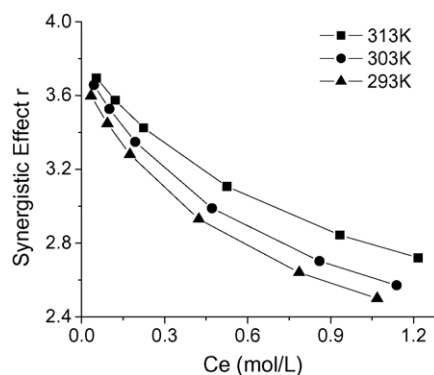

Fig. 4. Synergistic effect for the uptake of phenol on NDA103.

from aqueous solutions by NDA103, the synergistic effect r is introduced with the Eq. (7):

$$r = \frac{Q_e}{Q'_e} \qquad (7)$$

where Q_e is the experimental amount of phenol adsorbed on NDA103 at equilibrium (mmol/L); Q'_e (calculated as Q'_m by Eq. (4)) is the theoretical one without any synergistic or competitive effect (mmol/L); $r > 1$ indicates there is synergistic effect on adsorption. Fig. 4 describes the relation between the synergistic effect and the equilibrium concentration of phenol. The results at saturation are added in Table 5. As seen in Fig. 4 and Table 5, the values of r are always larger than 1, suggesting that synergistic effect exists in phenol adsorption on NDA103 under the conditions employed in this study. It also can be seen that the synergistic effect decreases as the equilibrium concentration increases, which is also probably attributed to the reduction in the adsorption sites and the augment of the electrostatic repulsion caused by the increase in the negative charge of adsorbed phenol.

4. Conclusions

The adsorption isotherms of phenol on nonpolar adsorbent XAD4, aminated adsorbent NDA103 and weak base adsorbent IRA96C can be fitted satisfactorily by Langmuir and Freundlich equations, which indicates a favourable and exothermic process. The adsorption capacity and adsorption affinity of NDA103 towards phenol were greater than that of XAD4 and IRA96C, which could be explained by the synergistic effect. During the phenol adsorption process on NDA103, because the total adsorption capacity is much more

than the sum of van der Waals interaction and hydrogen bonding interaction that occur individually, the two interactions occur simultaneously and synergistically. The synergistic effect decreased with the increased adsorption loading.

Acknowledgements

References

[1] Y. Ku, K.C. Lee, Removal of phenols from aqueous solution by XAD-4 resin, J. Hazard. Mater. 80B (2000) 59–68.

[2] A.M. Li, Q.X. Zhang, J.L. Chen, Z.H. Fei, C. Long, W.M. Li, Adsorption of phenolic compounds on Amberlite XAD-4 and its acetylated derivative MX-4, React. Funct. Polym. 49 (2001) 225–233.

[3] G.M. Gusler, T.E. Browne, Y. Cohen, Sorption of organic from aqueous solution onto polymeric resins, Ind. Eng. Chem. Res. 32 (1993) 2727–2735.

[4] R.S. Juang, J.Y. Shiau, Adsorption isotherms of phenols from water onto macroreticular resins, J. Hazard. Mater. 70B (1999) 171–183.

[5] R.S. Juang, J.Y. Shiau, H.J. Shao, Effect of temperature on equilibrium adsorption of phenols onto nonionic polymeric resins, Sep. Sci. Technol. 34 (1999) 1819–1831.

[6] Z.Y. Xu, Q.X. Zhang, C.L. Wu, L.S. Wang, G.K. Anderson, Adsorption of naphthalene derivatives on hypercrosslinked polymeric adsorbents, Chemosphere 38 (1997) 2003–2011.

[7] T. Karafil, J.E. Kilduff, Role of granular activated carbon surface chemistry on the adsorption of organic compounds 1. Priority pollutants, Environ. Sci. Technol. 33 (1999) 3217–3224.

[8] T. Karafil, M. Kitis, J.E. Kilduff, A. Wigton, Role of granular activated carbon surface chemistry on the adsorption of organic compounds 2. Natural organic matter, Environ. Sci. Technol. 33 (1999) 3225–3233.

[9] J.C. Crittenden, S. Sanmongraj, J.L. Bulloch, D.W. Hand, T.N. Rogers, T.F. Speth, M. Ulmer, Correlation of aqueous-phase adsorption isotherm, Environ. Sci. Technol. 33 (1998) 2926–2933.

[10] B.C. Pan, Y. Xiong, Q. Su, A.M. Li, J.L. Chen, Q.X. Zhang, Role of amination of a polymeric adsorbent on phenol adsorption from aqueous solution, Chemosphere 51 (2003) 953–962.

[11] V.A. Davankov, M.P. Tsyurupa, Structure and properties of porous hypercrosslinked polystyrene: the first representative of a new class of polymer network, React. Polym. 13 (1990) 27–42.

[12] M. Streat, L.A. Sweetland, Removal of pesticides from water using hypercrosslinked polymer phase. Part 1. Physical and chemical characterization of adsorbents, Trans. IChemE. B76 (1998) 115–126.

[13] P. Veverka, K. Jerabek, Mechanism of hypercrosslinking of chloromethylated styrene-divinylbenzene copolymers, React. Funct. Polym. 41 (1999) 21–25.

[14] S.H. Lin, C.P. Huang, Adsorption of hydrazoic acid from aqueous solution by macroreticular resin, J. Hazard. Mater. B84 (2001) 217–228.

[15] G.D. Liu, H.F. Yu, H.S. Yan, Z.Q. Shi, B.L. He, Utilization of synergetic effect of weak interactions in the design of polymeric sorbents with high sorption selectivity, J. Chromatogr. A 952 (2002) 71–78.

[16] H.M. Anasthas, V.G. Gaikar, Adsorption of acetic acid on ion exchange resins in non-aqueous conditions, React. Funct. Polym. 47 (2001) 23–35.

[17] D.R. Lide, Handbook of Chemistry and Physics, 80th ed., CRC Press, Boca Raton, 1991.

[18] F.L. Slejko, Adsorption Technology: A Step-by-Step Approach to Process Evaluation and Application, Marcel Dekker, New York, 1985.

[19] M. Goto, N. Hayashi, S. Goto, Adsorption and desorption of phenol on anion-exchange resin and activated carbon, Environ. Sci. Technol. 20 (1986) 463–467.

[20] R.A. Garcia-Delgado, L.M. Cotouelo-Minguez, J.J. Rodiguez, Equilibrium study of single-solute adsorption of anionic surfactants with polymeric XAD resins, Sep. Sci. Technol. 27 (1992) 975–987.